The Astrophysical Journal Letters, 723:L185–L189, 2010 November 10 doi:10.1088/2041-8205/723/2/L185

MAGNETIC LOOPS IN THE QUIET SUN

T. Wiegelmann[1], S. K. Solanki[1,2], J. M. Borrero[3], V. Martínez Pillet[4], J. C. del Toro Iniesta[5], V. Domingo[6], J. A. Bonet[4], P. Barthol[1], A. Gandorfer[1], M. Knölker[7], W. Schmidt[3], and A. M. Title[8]
[1] Max-Planck-Institut für Sonnensystemforschung, Max-Planck-Str. 2, 37191 Katlenburg-Lindau, Germany; wiegelmann@mps.mpg.de
[2] School of Space Research, Kyung Hee University, Yongin, Gyeonggi 446-701, Republic of Korea
[3] Kiepenheuer-Institut für Sonnenphysik, Schöneckstr. 6, 79104 Freiburg, Germany
[4] Instituto de Astrofísica de Canarias, C/Via Láctea s/n, 38200 La Laguna, Tenerife, Spain
[5] Instituto de Astrofísica de Andalucía (CSIC), Apartado de Correos 3004, 18080 Granada, Spain
[6] Grupo de Astronomía y Ciencias del Espacio, Universidad de Valencia, 46980 Paterna, Valencia, Spain
[7] High Altitude Observatory, National Center for Atmospheric Research,[9] Boulder, CO 80307, USA
[8] Lockheed Martin Solar and Astrophysics Laboratory, Bldg. 252, 3251 Hanover Street, Palo Alto, CA 94304, USA
Received 2010 June 7; accepted 2010 August 3; published 2010 October 15

ABSTRACT

We investigate the fine structure of magnetic fields in the atmosphere of the quiet Sun. We use photospheric magnetic field measurements from Sunrise/IMaX with unprecedented spatial resolution to extrapolate the photospheric magnetic field into higher layers of the solar atmosphere with the help of potential and force-free extrapolation techniques. We find that most magnetic loops that reach into the chromosphere or higher have one footpoint in relatively strong magnetic field regions in the photosphere. Ninety-one percent of the magnetic energy in the mid-chromosphere (at a height of 1 Mm) is in field lines, whose stronger footpoint has a strength of more than 300 G, i.e., above the equipartition field strength with convection. The loops reaching into the chromosphere and corona are also found to be asymmetric in the sense that the weaker footpoint has a strength $B < 300$ G and is located in the internetwork (IN). Such loops are expected to be strongly dynamic and have short lifetimes, as dictated by the properties of the IN fields.

Key words: Sun: chromosphere – Sun: corona – Sun: magnetic topology – Sun: photosphere

Online-only material: color figures

1. INTRODUCTION

The Sun's magnetic field lies at the heart of the heating of the solar corona and the solar chromosphere (with the possible exception of the basal flux; see, e.g., Bello González et al. 2010). Unfortunately, however, the magnetic field is measured almost exclusively in the solar photosphere and needs to be extrapolated from there in order to obtain its structure in the Sun's upper atmosphere. The balloon-borne Sunrise mission (Solanki et al. 2010; Barthol et al. 2010) obtained the magnetic field in the quiet solar photosphere with a very high and homogeneous spatial resolution. This allows us to investigate the three-dimensional structure of the quiet Sun's magnetic field in more detail as compared with *SOHO* (e.g., Wiegelmann & Solanki 2004; He et al. 2007) or *Hinode* (e.g., Martínez González & Bellot Rubio 2009; Martínez González et al. 2010).

The resolution of the extrapolated field in the vertical direction depends on the spatial scales of the photospheric measurements. With a pixel size of 40 km on the Sun and a spatial resolution of ∼100 km, we can, for the first time, resolve the thin layer of the photosphere and the lower chromosphere with several grid points. This allows us to study the magnetic connectivity between photosphere, chromosphere, and corona by well-resolved magnetic loops. We also briefly discuss the possible implications of our results for quiet-Sun loop heating models. This is of particular interest due to the large number of horizontal magnetic features in the photosphere, many of them associated with emerging magnetic loops (Martínez González et al. 2008; Danilovic et al. 2010), and the lack of acoustic wave energy flux proposed by Carlsson et al. (2007) which inspires us to consider alternatives, although the recent work by Bello González et al. (2009, 2010) suggests that the acoustic energy flux may well have been underestimated in the past due to insufficient spatial resolution.

2. EXTRAPOLATION OF PHOTOSPHERIC MAGNETIC FIELD MEASUREMENTS INTO THE UPPER SOLAR ATMOSPHERE

Here, we use a (phase diversity reconstructed) Stokes vector map of a 37 × 37 Mm quiet-Sun region in the photosphere recorded by Sunrise/IMaX (Martínez Pillet et al. 2010, the data set was observed for 1.616 hr starting at 00:00 UT on 2009 June 9). The magnetic vector is obtained by inverting these data using the VFISV code by Borrero et al. (2010). We take 200 km as the average height at which the Fe I spectral line at 5250.2 Å senses B, although it is difficult to define (Sanchez Almeida et al. 1996) and, in fact, varies from point to point over the solar surface. The height of this layer corresponds to $z = 0$ in Figure 1.

To get a first impression of the three-dimensional magnetic field structure in the chromosphere and corona, we extrapolate the photospheric measurements into the atmosphere under the force-free assumption:

$$\nabla \times \mathbf{B} = \alpha \mathbf{B} \tag{1}$$

$$\nabla \cdot \mathbf{B} = 0 \tag{2}$$

$$\mathbf{B} = \mathbf{B}_{\rm obs} \text{ in photosphere,} \tag{3}$$

where $\mathbf{B}$ is the magnetic flux density and α is the force-free parameter. Here, we mainly use potential field extrapolations

[9] The National Center for Atmospheric Research is sponsored by the National Science Foundation.

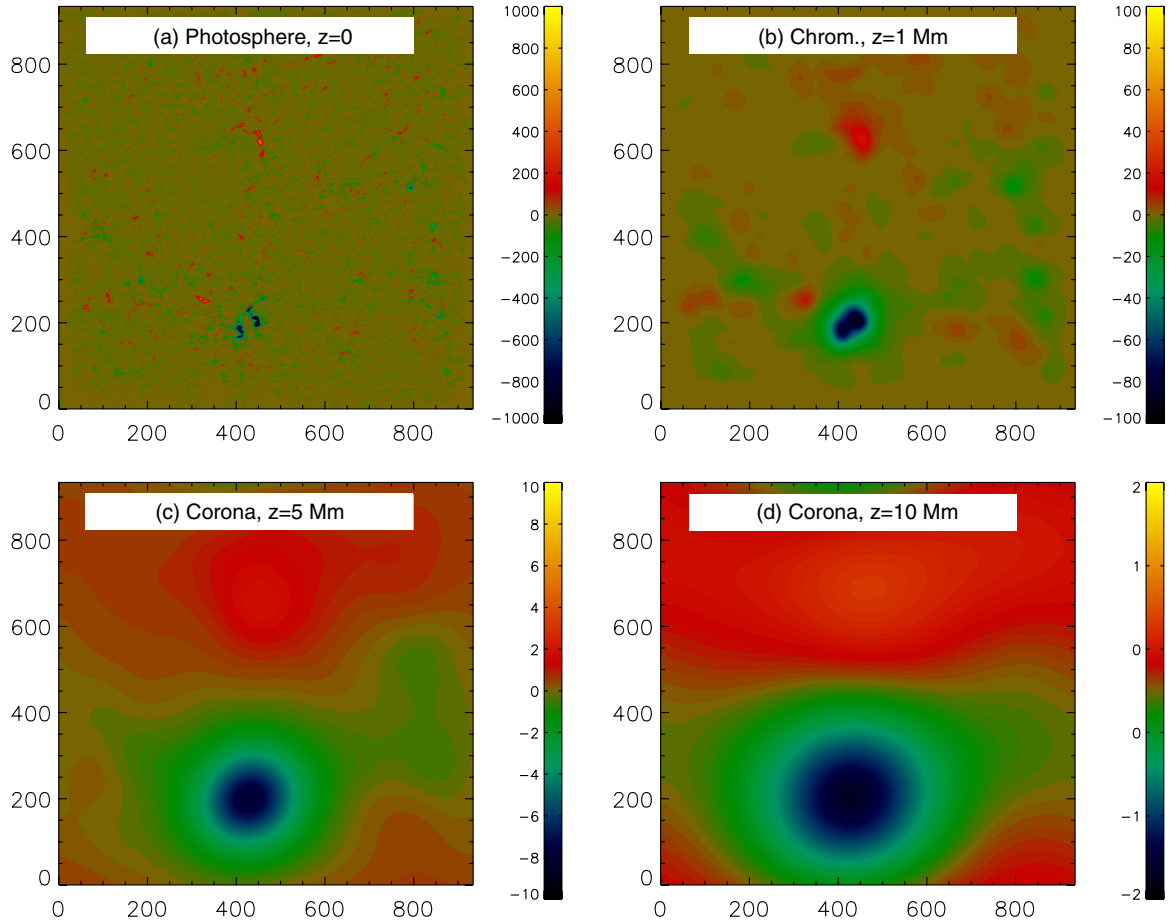

Figure 1. Vertical magnetic field at different heights. Panel (a) shows the measured magnetogram in the photosphere and panels (b)–(d) shows the vertical magnetic field distribution in different heights in the solar atmosphere, as reconstructed with a potential field model. The color bars show the magnetic field strength in G.
(A color version of this figure is available in the online journal.)

($\alpha = 0$) due to the generally low signal level in the quiet Sun, particularly linear polarization. Taking into account the non-force-free character of photosphere and lower chromosphere (as, e.g., proposed in Petrie & Neukirch 2000; Wiegelmann & Neukirch 2006) requires information on the plasma density and temperature distribution. The employed approximation is supported by spectro-polarimetric observations from Martínez González et al. (2010), which suggest that quiet-sun loops show a potential-field-like structure. We solve Equations (1)–(3) with the help of a fast Fourier approach (see Alissandrakis 1981) with the measured vertical magnetic field as boundary condition. A Fourier approach is justified because the magnetogram is almost flux balanced with $\sum_{x,y} B_z / \sum_{x,y} |B_z| = -0.077$. The computations are carried out in a cubic box with $936 \times 936 \times 468$ grid points in x, y, z, where z is the vertical direction. We use a constant grid resolution of 40 km in each direction, which corresponds to a total three-dimensional model volume of $37 \times 37 \times 19$ Mm. Figure 1(a) shows the line-of-sight photospheric magnetic field and Figures 1(b)–(d) show slices of the reconstructed magnetic field at different heights in the solar atmosphere. With increasing height in the solar atmosphere the magnetic field becomes smoother and shows a dipolar structure at coronal heights.

3. STATISTICS OF MAGNETIC LOOPS

We compute magnetic field lines from all pixels above a certain threshold value, here $|B_z| > 30$ G in the photosphere, which corresponds to the 3σ noise level of the magnetogram. The field line integration is started in a rectangular area at the center of the magnetogram, 150 pixels or 6 Mm away from the lateral boundaries. A total of 28,005 field lines are followed from one footpoint to the other. Of these, 1936 (7%) leave the computational domain through the lateral or top boundaries. We cannot say if these lines are really open or closed outside the SUNRISE/IMaX field of view (FOV). Consequently, we do not consider them further in this section. For simplicity, we call closed magnetic field lines "loops" for the rest of this Letter. Such magnetic loops are ubiquitous in the solar atmosphere, although only a fraction of these loops might be visible in images made in chromospheric, transition region or coronal radiation. Loops with a height of less than 100 km (9321, 33% of all field lines) may not be sufficiently spatially resolved and are not considered further, leaving 16,748 field lines (60% of all) to be studied.

Figure 2(a) shows a randomly chosen fraction of 2% of these loops and Figure 2(b) shows a histogram of the loop height distribution for all resolved loops. The average loop height is 1.24 ± 2.45 Mm.[10] The number of small loops (below about 1 Mm) is significantly larger than that of higher loops. Fifty-one percent of the resolved loops[11] close within photospheric heights

[10] For higher (lower) threshold values of $|B_z|$, the number of small loops decreases (increases), which affects the average loop height, e.g., to 1.38 Mm and 1.09 Mm for a threshold of 40 G and 20 G, respectively.
[11] All loops higher than 100 km, including the ones not closing within the SUNRISE/IMaX FOV.

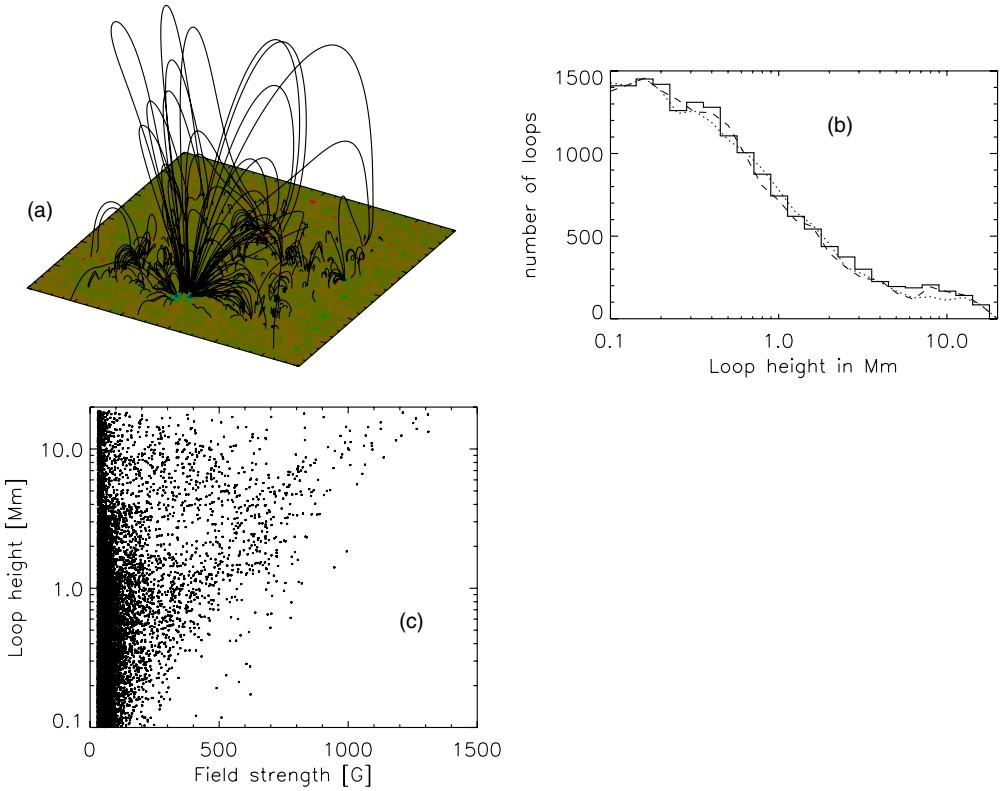

Figure 2. (a) Random selection of 2% of magnetic loops, computed from a potential field reconstruction. (b) Loop statistics for all resolved loops. The solid histogram-style line corresponds to a potential field, and the dotted and dashed lines to a linear force-free model with $\alpha \cdot L = 4$ and -4, respectively. (c) Scatter plot of loop height vs. leading footpoint vertical field.

(A color version of this figure is available in the online journal.)

(<500 km) and 29% in the chromosphere (500–2500 km). Finally, 20% of the loops reach into the corona (>2500 km), but half of these long coronal loops do not close within the Sunrise FOV.

We also investigated how using a linear force-free model instead of a potential field model influences the loop height statistics. These models contain the force-free parameter α, which cannot be deduced from the available data. Consequently, one unique linear force-free model cannot be computed. To investigate the influence of linear electric currents, we carried out computations with $\alpha L = \pm 4$, respectively, where $L = 37$ Mm is the size of the employed portion of the magnetogram (see dotted and dashed lines in Figure 2(b), respectively); 4 is already quite a large value for the normalized force-free parameter αL and close to the mathematically allowed maximum value of $|\alpha L| = \sqrt{2}\pi$ (see discussion in Seehafer 1978, for a suitable rank of α-values for linear force-free models). As visible in Figure 2(b), the loop height statistics are almost identical to those obtained from potential fields. Small differences occur only for field lines higher than about 5 Mm. For our study, which mainly concentrates on lower chromospheric loops, it is therefore justified to consider only potential fields.

Figure 2(c) contains a scatter plot of loop height versus magnetic field strengths at the leading footpoint, i.e., the footpoint with the largest field strength. It shows that loops of any height can begin from weak fields, but only long loops start from strong-field footpoints. This means that the stronger field ($|B_z| \gtrsim 800$ G) loops are all long enough to reach into the solar corona, whereas the apex of a loop originating in a weaker field region can lie in the photosphere, chromosphere, or corona.

4. ON THE ORIGIN OF CHROMOSPHERIC MAGNETIC FIELDS AND MAGNETIC ENERGY

In the following, we investigate in more detail the origin of magnetic fields in the mid-chromosphere at a height of 1 Mm and are particularly interested in the magnetic connectivity with photospheric fields. To this aim we start the magnetic field line integration in the chromosphere (see Figure 1(b)) at every pixel except in a layer of 150 pixels toward the magnetogram boundaries. We track all field lines down to the photosphere and determine here in particular the leading, stronger photospheric footpoints.[12] From this footpoint map, we can then distinguish between photospheric pixels hosting magnetic loops reaching into the chromosphere or higher and pixels not hosting such loops. Figure 3(a) shows the magnetic field strength distribution $|B_z|$ in the photosphere. The solid line is for all pixels, the dashed line for pixels hosting footpoints of field lines that reach to a height of at least 1 Mm, and the dotted line is for pixels not hosting such loops. Above 500 G, the solid and dashed lines are practically identical and nearly all pixels above 500 G host footpoints of chromospheric loops. For weak fields (<100 G), only about 2% of the pixels host chromospheric loops, but the total number of these (hosting) pixels is still more than one order of magnitude higher than strong-field pixels. This raises the question, which photospheric fields can influence the chromospheric and coronal gas more strongly, the few regions with strong fields or the many regions with

[12] Some long field lines do not close within the SUNRISE FOV and for them we can only identify one footpoint. For the analysis in this section, these field lines are included in the statistics assuming that the known footpoint is the stronger one. The relation to the weaker footpoints is investigated in Section 5.

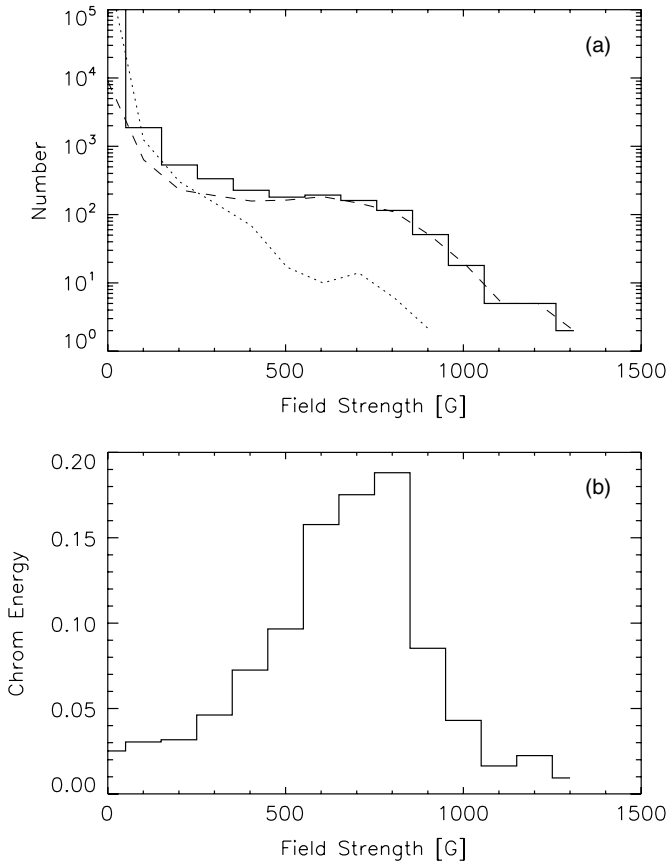

Figure 3. (a) Photospheric field strength $|B_z|$ statistics of the photospheric magnetogram (excluding the 150 pixel layer toward the boundaries). The solid histogram-style line corresponds to all photospheric pixels, the dashed line to pixels hosting footpoints of field lines reaching at least to 1 Mm, i.e., into the mid-chromosphere, and the dotted line corresponds to pixels not hosting such field lines. (b) Histogram showing the fraction of magnetic energy at a height of 1 Mm (mid-chromosphere) in loops with a particular field strength of their leading footpoint.

weak fields? To answer this question, we compute the magnetic energy at a height of 1 Mm and investigate which fraction of the energy is magnetically connected to photospheric footpoints with a particular field strength. As one can see in Figure 3(b) the weak photospheric fields (<100 G) hardly contribute to chromospheric magnetic energy. In addition, although only 0.91% of all photospheric pixels have a field strength above 100 G, they are connected to 97% of the chromospheric magnetic energy. The 0.32% of pixels above the equipartition field strength of 300 G contribute to 91% of the chromospheric magnetic energy. At the equipartition field strength (which is in the range of 200–400 G in the photosphere; see, Solanki et al. 1996), the magnetic energy is identical to the energy of the convective flow. The equipartition field strength has relevance for quiet-Sun magnetic features, because magnetic flux tubes need to have a larger field strength in order to survive as a distinct feature. It is therefore natural to distinguish network elements from internetwork (IN) features by the equipartition field strength. Here, we used the average value of 300 G.

Note that the photospheric field strength values are based on single component inversions assuming spatially resolved fields and are consequently lower limits (for the stronger field, they are close to the true value; see Lagg et al. 2010), and so are the above energy fractions of the chromospheric magnetic energy. The above numbers refer to the leading (stronger) footpoint.

5. RELATION BETWEEN THE TWO FOOTPOINTS OF MAGNETIC LOOPS

In the last section, we learned that 91% of the mid-chromospheric magnetic energy is topologically connected to photospheric footpoints with superequipartition field strength. However, still unknown is if both footpoints of long chromospheric and coronal loops have similar field strength or if it can be very different. If the latter is the case, this would also mean that the multiple field lines starting within the area of a strong magnetic pixel will end in many, possibly widely distributed weak-field pixels.[13] In Figure 4(a), we show a scatter plot of weak footpoint strength versus strong footpoint strength.[14] Ninety-five percent of all loops with a leading foot strength of >300 G have the other footpoint in regions with <300 G. Figure 4(b) shows the photospheric vertical field $|B_z|$ statistics for pixels hosting a leading (stronger) footpoint (solid histogram-style line) and for pixel hosting a weak footpoint (dashed line). Obviously, the vertical field of both footpoints for long loops (reaching at least into the chromosphere) is very different. Partly,

[13] In order to fulfill $\nabla \cdot \mathbf{B} = 0$, we get the relation $B_1 A_1 = B_2 A_2$ for the footpoint areas A_1 and A_2 of magnetic flux tubes containing a bundle of field lines.

[14] Necessarily, we had to exclude those field lines which do not close within the SUNRISE FOV, because we cannot identify both footpoints for them.

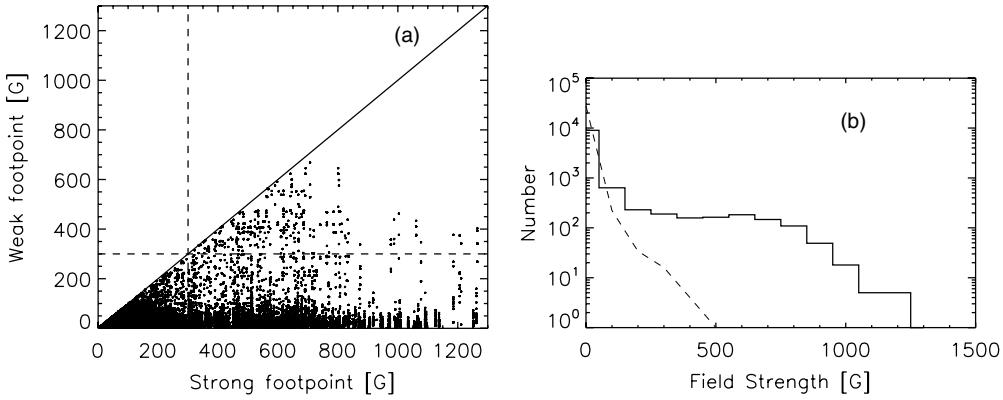

Figure 4. Relation between strong and weak footpoints of magnetic loops which reach at least into the chromosphere. Excluded have been loops that do not close within the SUNRISE FOV (14%), because the strength of one footpoint remains unknown. Panel (a) shows a scatter plot of weak footpoint strength vs. strong footpoint strength. The solid diagonal line corresponds to equal strength of both footpoints and the dashed horizontal and vertical lines mark the equipartition field strength of 300 G. Panel (b): photospheric field strength $|B_z|$ statistics for the strong (solid line) and weak footpoints (dashed line) of chromospheric and coronal loops.

this has to do with the different field strength distribution in the two magnetic polarities for this particular magnetogram. The maximum vertical field in the negative field region is 1311 G, compared to 707 G in positive polarity regions.[15] Investigations of further quiet-Sun regions with high resolution are necessary to see if such different field strengths are common or an exception (for quiet-Sun investigations of magnetic flux, see, e.g., Wang et al. 1995).

6. CONCLUSIONS AND OUTLOOK

We investigated the small-scale structure of magnetic fields in the solar atmosphere with emphasis on the magnetic connectivity between the photosphere and chromosphere. We found that chromospheric areas containing about 91% of the magnetic energy are topologically connected to a photospheric footpoint with a strength above 300 G, i.e., with an energy density higher than the average equipartition with that of convective flows. For the majority of the loops, the magnetic field strength in both footpoints differs significantly, with the second footpoint having a field strength below equipartition, i.e., network elements connect magnetically mainly to IN features, in general agreement with numerical experiments of Schrijver & Title (2003) and Jendersie & Peter (2006). An interesting question is to what extent the finding that network elements are connected mainly with IN features might influence models of quiet-Sun loop heating (e.g., Hansteen 1993; Chae et al. 2002; Müller et al. 2003, 2004). Such loop heating models usually assume a constant cross section, an approximation which is not fulfilled for field lines connecting strong and weak field regions in the photosphere. It is also worth noting that IN fields are more dynamic and short lived than network fields (IN field average lifetimes are about 10 minutes according to de Wijn et al. 2008). Since most chromospheric and coronal loops, at least in the observed region, are connected at one footpoint with IN fields, we expect the chromospheric and coronal field to be more dynamic than suggested by network fields alone. Time series of high-resolution magnetograms in the quiet Sun can be used to investigate this further and to revisit coronal recycling (e.g., as investigated at much lower spatial resolution by Close et al. 2004, 2005).

The German contribution to SUNRISE is funded by the Bundesministerium für Wirtschaft und Technologie through Deutsches Zentrum für Luft- und Raumfahrt e.V. (DLR), Grant No. 50 OU 0401, and by the Innovationsfond of the President of the Max Planck Society (MPG). The Spanish contribution has been funded by the Spanish MICINN under projects ESP2006-13030-C06 and AYA2009-14105-C06 (including European FEDER funds). The HAO contribution was partly funded through NASA grant NNX08AH38G. This work has been partially supported by the WCU grant R31-10016 funded by the Korean Ministry of Education, Science, and Technology.

REFERENCES

Alissandrakis, C. E. 1981, A&A, 100, 197
Barthol, P., et al. 2010, Sol. Phys., in press (arXiv:1009.2689)
Bello González, N., Flores Soriano, M., Kneer, F., & Okunev, O. 2009, A&A, 508, 941
Bello González, N., et al. 2010, ApJ, 723, L134
Borrero, J. M., et al. 2010, Sol. Phys., 35
Carlsson, M., et al. 2007, PASJ, 59, 663
Chae, J., Poland, A. I., & Aschwanden, M. J. 2002, ApJ, 581, 726
Close, R. M., Parnell, C. E., Longcope, D. W., & Priest, E. R. 2004, ApJ, 612, L81
Close, R. M., Parnell, C. E., Longcope, D. W., & Priest, E. R. 2005, Sol. Phys., 231, 45
Danilovic, S., et al. 2010, 723, L149
de Wijn, A. G., et al. 2008, ApJ, 684, 1469
Hansteen, V. 1993, ApJ, 402, 741
He, J., Tu, C., & Marsch, E. 2007, A&A, 468, 307
Jendersie, S., & Peter, H. 2006, A&A, 460, 901
Lagg, A., et al. 2010, ApJ, 723, L164
Martínez González, M. J., & Bellot Rubio, L. R. 2009, ApJ, 700, 1391
Martínez González, M. J., Collados, M., Ruiz Cobo, B., & Beck, C. 2008, A&A, 477, 953
Martínez González, M. J., Manso Sainz, R., Asensio Ramos, A., & Bellot Rubio, L. R. 2010, ApJ, 714, L94
Martínez Pillet, V., et al. 2010, Sol. Phys., in press (arXiv:1009.1095)
Müller, D. A. N., Hansteen, V. H., & Peter, H. 2003, A&A, 411, 605
Müller, D. A. N., Peter, H., & Hansteen, V. H. 2004, A&A, 424, 289
Petrie, G. J. D., & Neukirch, T. 2000, A&A, 356, 735
Sanchez Almeida, J., Ruiz Cobo, B., & del Toro Iniesta, J. C. 1996, A&A, 314, 295
Schrijver, C. J., & Title, A. M. 2003, ApJ, 597, L165
Seehafer, N. 1978, Sol. Phys., 58, 215
Solanki, S. K., Zufferey, D., Lin, H., Rüedi, I., & Kuhn, J. R. 1996, A&A, 310, L33
Solanki, S. K., et al. 2010, ApJ, 723, L127
Tarbell, T. D., & Title, A. M. 1977, Sol. Phys., 52, 13
Wang, J., Wang, H., Tang, F., Lee, J. W., & Zirin, H. 1995, Sol. Phys., 160, 277
Wiegelmann, T., & Neukirch, T. 2006, A&A, 457, 1053
Wiegelmann, T., & Solanki, S. K. 2004, Sol. Phys., 225, 227

[15] Indirect evidence of large network fields of 1–2 kG concentrated in small regions has already been given in Tarbell & Title (1977), but the magnetograph resolution of that time has been too low to resolve such structures.